Pender, Gareth; Néelz, Sylvain

Hydrodynamic Floodplain Modelling in the Urban Area Using Remotely Sensed Digital Elevation Models

HYDRODYNAMIC FLOODPLAIN MODELLING IN THE URBAN AREA USING REMOTELY SENSED DIGITAL ELEVATION MODELS

Gareth Pender[1] and Sylvain Néelz[2]

[1] Professor, School of the Built Environment, Heriot Watt University
Edinburgh, UK, e-mail:g.pender@hw.ac.uk
[2] Lecturer, School of the Built Environment, Heriot Watt University
Edinburgh, UK, e-mail:s.p.f.neelz@hw.ac.uk

ABSTRACT

The paper will report on a co-ordinated programme of research on the use of 2D hydrodynamic models to predict overland flood flow in the urban area. Three aspects of model application will be considered. Firstly, errors in model predictions arising from errors in the underlying DEM are assessed and quantified. In some cases these errors can result in significant changes in predicted final or maximum inundation extent and water levels. Secondly, a case study to demonstrate a technique for using the roughness parameter in 2D coarse-grid inundation models to represent sub-grid scale effects caused by buildings on urban floodplains is presented. In this method the roughness is assigned on a cell-by-cell basis depending on the percentage of surface area covered by buildings in each cell. Finally, results from Coarse Grid Models (CGM) at grid resolutions of 10m and 50m will be compared against benchmark results from a Fine Grid Model (FGM) at 2m grid resolution using statistics based on the timing of inundation throughout the modelled domain. Methods for improving the coarse grid predictions using simulations from a limited number of fine grid simulations will be presented and illustrated by application to a case study site.

Keywords: digital elevation models, two-dimensional hydrodynamic modelling

1. INTRODUCTION

Until relatively recently, most flood modelling in the UK was undertaken using 1D modelling methods. However, the increasing availability of remotely sensed digital elevation models of both rural and urban floodplains has resulted in an increased interest in the use of 2D modelling, or in some cases hybrid techniques where a 1D model for the river channel is linked to 2D flood plain models.

The paper reports on two challenges arising from the application of 2D models to flood inundation problems. Firstly, the extent to which errors in the remotely sensed DEM impact on model predictions, and secondly, the compromise between model grid resolution and runtime necessary to ensure predictions can be made using typical desk top computing facilities. In the later inclusion of sub-grid scale blockage in relatively coarse grid models and improving coarse grid model results are discussed.

2. THE INFLUENCE OF ERRORS IN DEMS ON MODEL PREDICTIONS

Since around 1994, the modelling of flood inundation patterns and flow routes on floodplains has made increasing use of high-resolution Digital Terrain Models (DTMs)

obtained from Light Detection And Ranging (LiDAR) technology. The suitability of LiDAR for such applications has been extensively investigated (Gomes Pereira and Wicherson 1999, Marks & Bates 2000, Cobby *et al* 2003), but there is little information on the influence of errors and uncertainties in LiDAR digital elevation data on the quality of predictions made by hydraulic models.

Néelz and Pender (2006) report on differences in computer simulations of an identical flood event carried out using three digital elevation models: a benchmark high-resolution DEM and two DEMs based on the benchmark but containing perturbations introduced to mimic errors found in LiDAR data sets. The DEMs are referred to as DEM 1, 2 and 3 respectively, Table 1 and Figure 1. A hydraulic model was constructed using each DEM and predictions of flow route, velocity, depth and inundation timing were compared for simulations generated from a consistent set of boundary conditions.

	σ_V	σ_H
DEM2	0.05 m	0.15 m
DEM3	0.10 m	0.30 m

Table 1. Vertical and horizontal Error standard deviations used in Building DEM 2 and DEM 3.

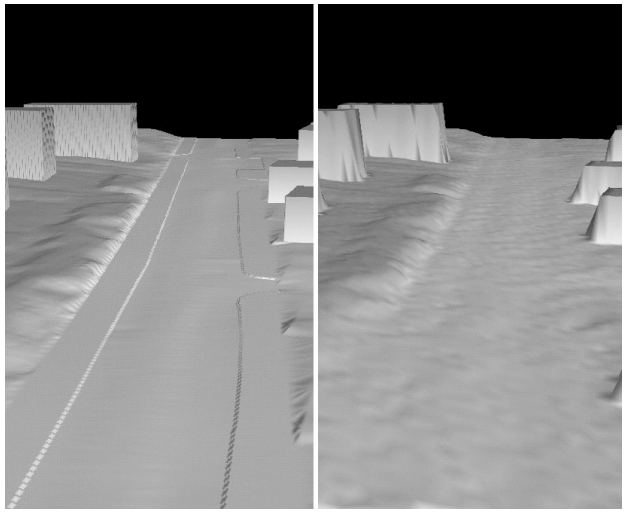

Figure 1. Sample of DEM1 (left) and the corresponding view in DEM3.

2.1 Model construction

The simulated flood occurred in a ~0.5 km^2 area in Greenfield, a suburb of Glasgow, UK (Figure 2). A TUFLOW 2D model was used to obtain computer predictions. TUFLOW solves the shallow-water equations to simulate river flow and flood propagation on a regular square mesh using the Stelling finite difference, alternating direction implicit (ADI) scheme (Stelling (1984), adapted for upstream controlled flow regimes by Syme (1991).

The model used a flow vs. time upstream boundary condition at the location indicated in Figure 2 and a water level vs. time downstream boundary condition at a location outside Figure 2. The grid size used was 2 m with Manning's roughness values of 0.015 on paved surfaces (roads, pavement and footpaths) and 0.05 on all other areas. Grid cell elevations (which included the geometry of buildings) were taken directly from the underlying DEMs. Results were output as flood depth maps at specified times, or as time series at the locations indicated in Figure 2.

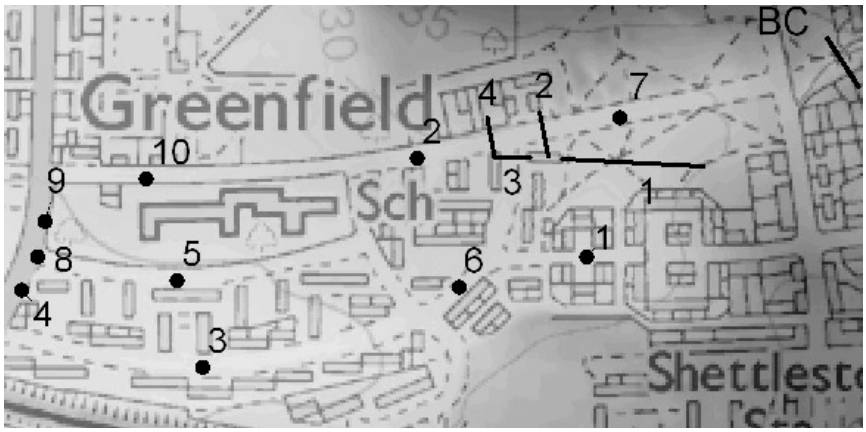

Figure 2. TUFLOW model of Greenfield. Locations of the upstream boundary condition and of 10 output points (velocity and free surface elevation) and 4 output lines (flow discharge). (© Crown Copyright Ordnance Survey. An EDINA Digimap / JISC supplied service.)

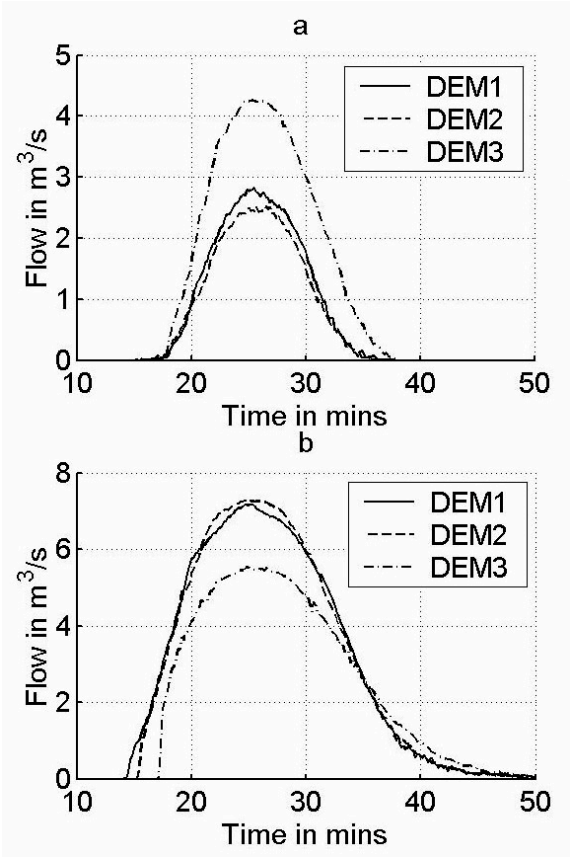

Figure 3. Results from initial simulations with DEM1 DEM2 and DEM3
Time series of discharges Q1 (a) and Q2 (b).

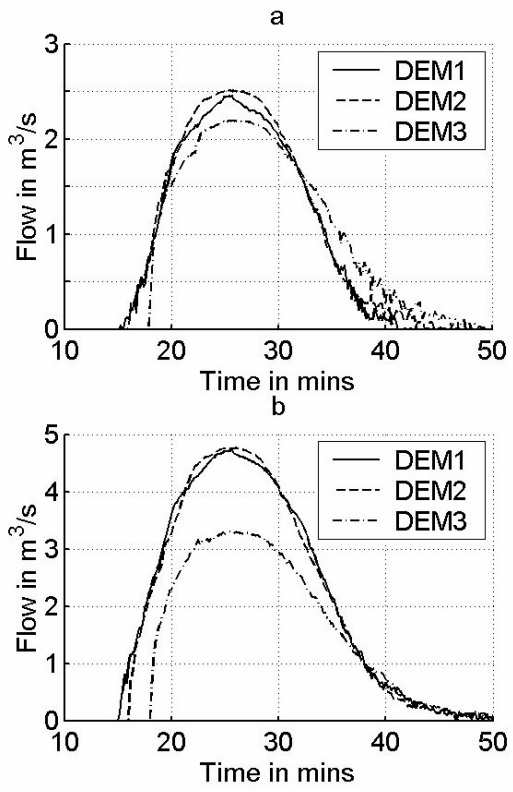

Figure 4 Results from initial simulations with DEM1, DEM2 and DEM3.
Time series of discharges Q3(a) and Q4(b).

2.2 Influence of DEM errors on model predictions

A visual comparison of maps of inundation extent indicated that the errors had little effect on the extent of inundation. However, a significant impact on the flow distribution between the different routes was observed particularly in the case of DEM 3. This was

assessed by comparing the discharges flowing through lines 1 to 4 on Figure 2. These discharges are referred to as Q1 through to Q4, for which time series are shown in Figures 3 and 4. Peak values of discharges differed by 11 % the case of DEM 2 (Fig. 3a). In the case of DEM 3, the proportion of the flow flowing southwards (Q1) instead of westwards (Q2) increased from ~28 % to ~44 %. The topography of this particular study area meant that flood water came to rest in a "pond" located in the lower part of the catchment (southwest quarter of Figure 2), as a consequence no significant difference in final water level was observed at this location (Fig. 5a). The effects of LiDAR errors in terms of modelled flow velocities were difficult to assess because they resulted from complex interactions between several factors.

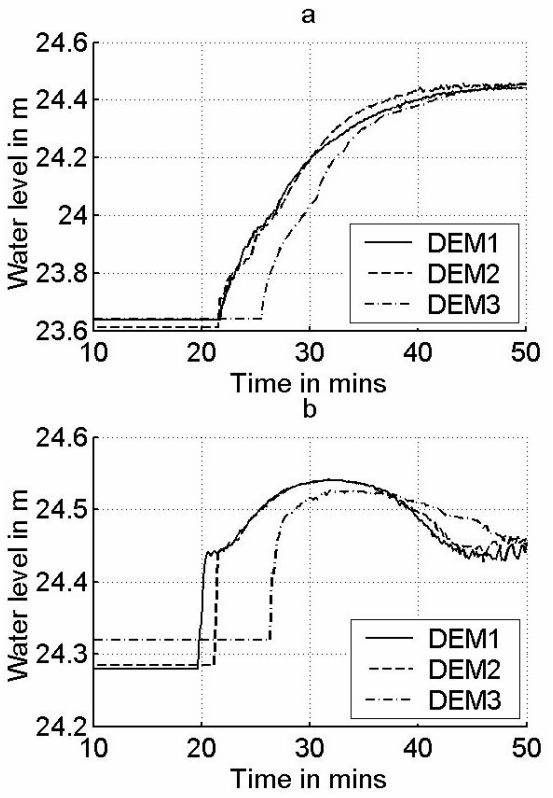

Figure 5. Free surface elevation vs.time at locations 3 (a) and 4 (b).

3. REPRESENTATION OF SUB-GRID SCALE BLOCKAGE

The plan dimensions of the above study area made it possible to undertake the hydrodynamic simulations on a high resolution (2 m) square grid while maintaining a reasonable simulation time using standard office computing facilities. This is not always possible and for larger study areas and a compromise is required between model resolution and simulation time. In such cases, representing buildings and other obstructions to flow within the computer grid becomes an issue, as the coarser grid (necessary to maintain practical simulation times) degrades representation of topographical features. In the following we investigate the use of the roughness parameter to account for sub-grid scale obstructions to flow in hydrodynamic models of urban areas.

3.1 Case study site

Here the study site is a ~5 km^2 area of lowlands along the banks of the Thames

Estuary in England. It is generally very flat, with most areas lying at only 1 m above Datum. A 1m (resolution) LiDAR Digital Terrain Model (filtered to remove vegetation and building features) provided the underlying topography used in the study. This DTM was further processed to remove "false blockages" such as bridges, and to fill in areas of missing data. In addition, exact building locations and geometries were extracted from Ordnance Survey (the mapping agency for Great Britain) Mastermap® data.

3.2 Model construction

An inflow hydrograph was used as an upstream boundary condition at the location indicated by an arrow in Figure 6. The shape of the hydrograph is similar to what could be expected for tidally driven inundation through a breached embankment. Inflow lasts for a few hours and ends as the tide recedes. Three grid resolutions were used (2m, 10m and 50m), and simulations were repeated with four different hydrographs of similar shapes, but characterised by a different value of the peak discharge, see Figure 7.

Figure 7: Map of the floodplain

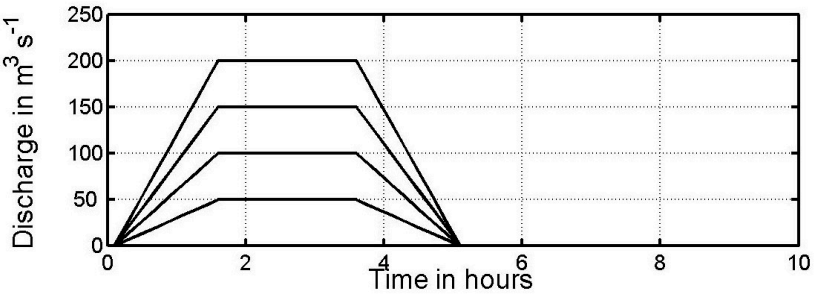

Figure 8: Inflow hydrographs used in the study

3.3 Fine grid model (FGM)

Ground elevations at computational nodes were extracted from the underlying DTM. In contrast with some previous studies (Néelz and Pender 2006), buildings were not reinstated into the DTM. Instead, the blockage effect that they exert on the flow was taken into account through the use of a very high Manning's 'n' value of 0.5 in computational cells found to coincide with buildings. This ensured that the flow velocities were reduced to near-zero values inside these cells. A value of Manning's 'n' of 0.035 was used uniformly in the rest of the domain.

3.4 Coarse grid model (CGM)

In the CGMs (resolutions 10m and 50m), node elevations were extracted from the DTM as in the FGM. However, as buildings only partially filled cells roughness values were assigned according to:

$$n = 0.035 + (0.075556 \cdot (k-1) + 0.16) \cdot p/100 \qquad \text{Equation (1)}$$

where p is the percentage of cell surface area occupied by buildings, and k is an integer. Ten simulations were run with $k=1,...,10$, so that k was the "calibration" parameter on which the agreement between FGM and CGM results depended.

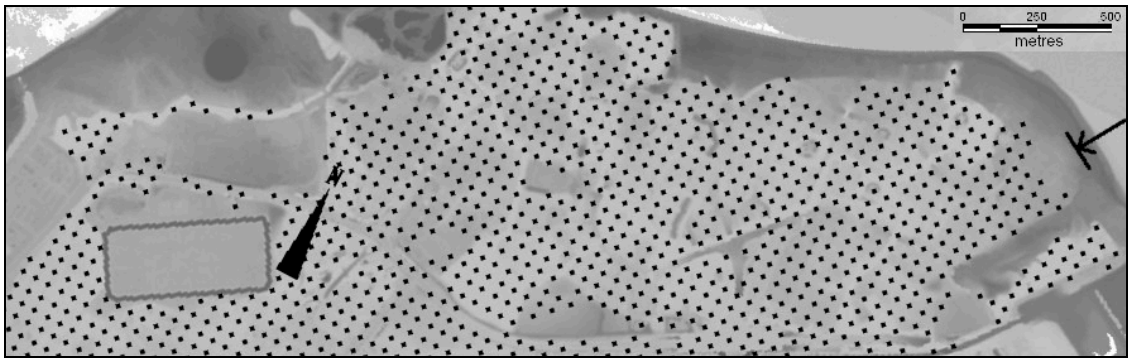

Figure 8 Output points

3.5 Optimising CGM predictions

The purpose of the modelling exercise is therefore to optimise the value of k (for 10m and 50m grid models) to minimise the differences between CGMs and the FGM across the solution domain. Differences between models were measure using the lag time 'T' for predicted values to reach a predetermined value of water depth 'H' or hazard coefficient (defined as $H=d.(v+0.5)$, in which v is the flow velocity). An optimum value of k was considered to have been identified when the mean of the differences T was zero and the standard deviation Σ of the differences was a minimum.

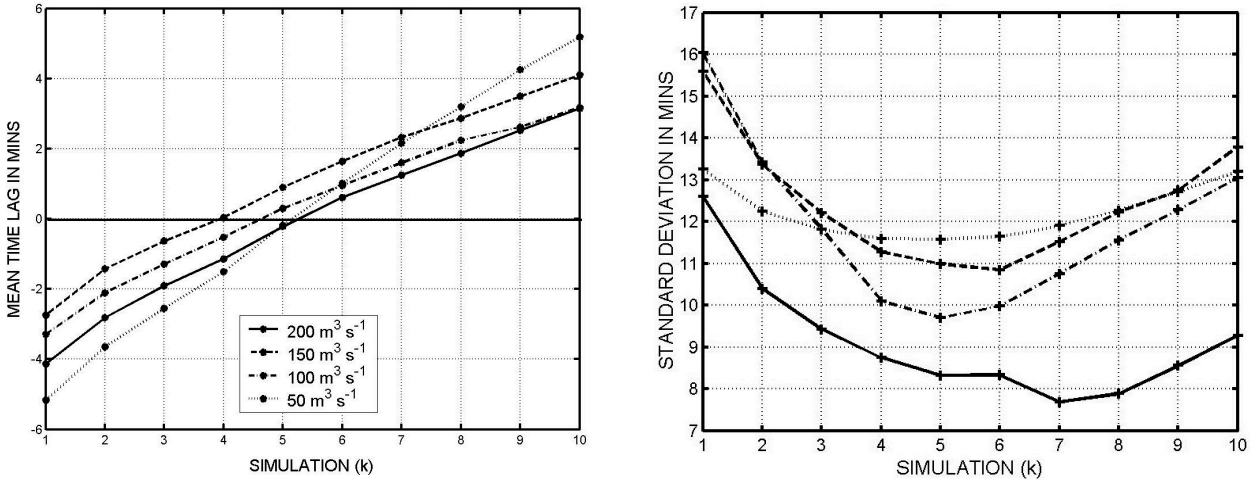

Figure 9 Plots of a) T vs. k and b) Σ vs. k for the 10m CGM, using arrival times based on water depth, also showing the dependency on the choice of threshold depth

The main conclusion is that an optimised value of k (within the interval 4-6) is clearly identifiable (Figure 9) for the 10m CGM. This varies only to a limited extent with the magnitude of the flood discharge. Results from the 50m CGM lead to similar conclusions, with optimised values of k being found in the same range.

4. IMPROVING CGM PREDICTIONS

The main advantage of utilising 2D hydrodynamic models is to obtain detailed prediction of the velocity field as the flood propagates across the floodplain. This is important as velocity is a key component of flood hazard. A further aspect of the research was therefore to investigate improving CGM estimates of velocity using a limited number (preferably no more than two) FGM predictions for each potential breach location. To investigate the potential of the method, further analysis of the results from the Thamesmead study was undertake using the data from the output points shown on Figure 8.

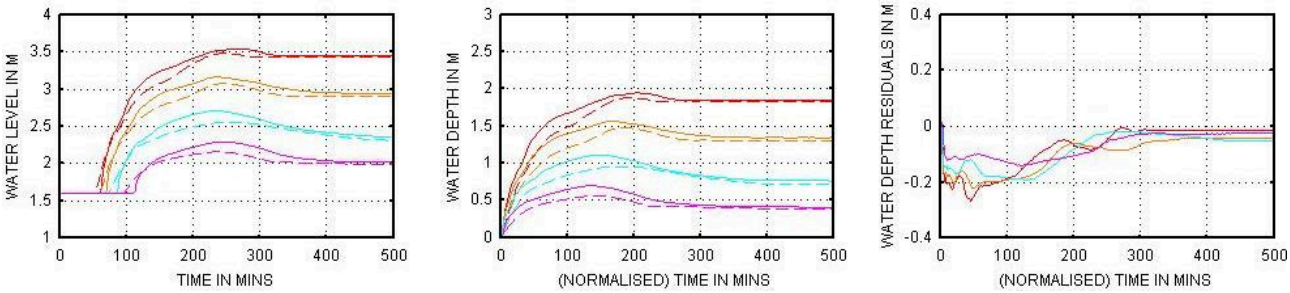

Figure 10. Reparameterisation of the time series (left) to the arrival time of the flood wave (centre). Solid lines: CGM results. Dashed lines: FGM results. The colours represent different values of q.

4.1 Prediction improvement technique

The technique progresses by:

1. Obtaining FGM and CGM predictions for high and low values of peak inflow through the breach location, here values of 100 m^3/s and 500 m^3/s are used.
2. As time series of predictions at almost all output points included a single discontinuity at the time of arrival of the flood wave (Figure 10(a)), it is necessary to first normalised to the arrival time of the flood wave.
3. Residual differences between FGM and CGM predictions at each output point are then calculated.
4. Other CGM simulations are undertaken for a different value of peak inflow (in the example presented here 50 m^3/s, 200 m^3/s and 350 m^3/s) these are then adjusted using linear interpolation or extrapolation of the residual values to bring them closer to the predictions that would be made from a FGM with this boundary condition.
5. The time lag is then reinstated into the prediction by reversing step 2.

4.2 Results

Figures 11 and 12 give an illustration of what can be achieved for time series predictions of water level and flows at two locations on the floodplain. The CGM predictions (light blue) have been corrected (red) to bring them closer to those of a FGM using the same boundary condition. Similar promising improvements are made at many other locations.

However, a number of limitations of the approach were also apparent as many results suffered from a) over- or under-correction for at least a part of the time domain, or b) arrival time prediction errors. The most important limitation occurred at locations where flooding was shallow or nonexistent for the training run q = 100 m^3/s. Also, residuals during the first minutes of the inundation process were often excessively dependent on q, as differences in the way topography is represented in the FGM and the CGM affect shallow flows only (and therefore have consequences for low values of q that last longer than for high values of q). This can cause noisy predictions of velocity during the rising limb of the flood, see Figure 12 (left), and can also lead to substantial errors in the arrival time predictions. In addition, the approach did not take into account how temporal characteristics of flood fronts varied depending on q. An example is shown in Figure 12 (right), where prediction inaccuracies for q = 200 m^3/s and q = 350 m^3/s between the times 150 and 300 min may be due to this. Predictions for q =50 m^3/s were very inaccurate at all locations where inundation was very shallow, see Figure 12 (left). Finally, it should be mentioned that the prediction of velocity was often made more difficult by the presence of oscillations (either physical or numerical) in the results from the training runs.

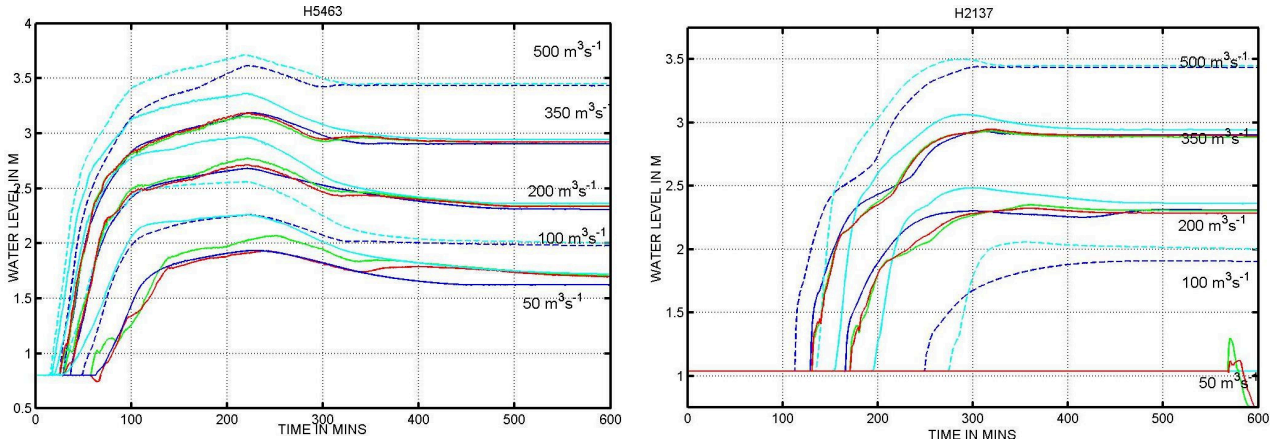

Figure 11. Prediction of water level at 2 locations on the floodplain. Training runs based on q = 100 m^3/s and q = 500 m^3/s. Methods used: linear interpolation/extrapolation of residuals (red); averaging of residuals (green). Light blue: CGM results. Dark blue: FGM results. Dashed lines: training runs

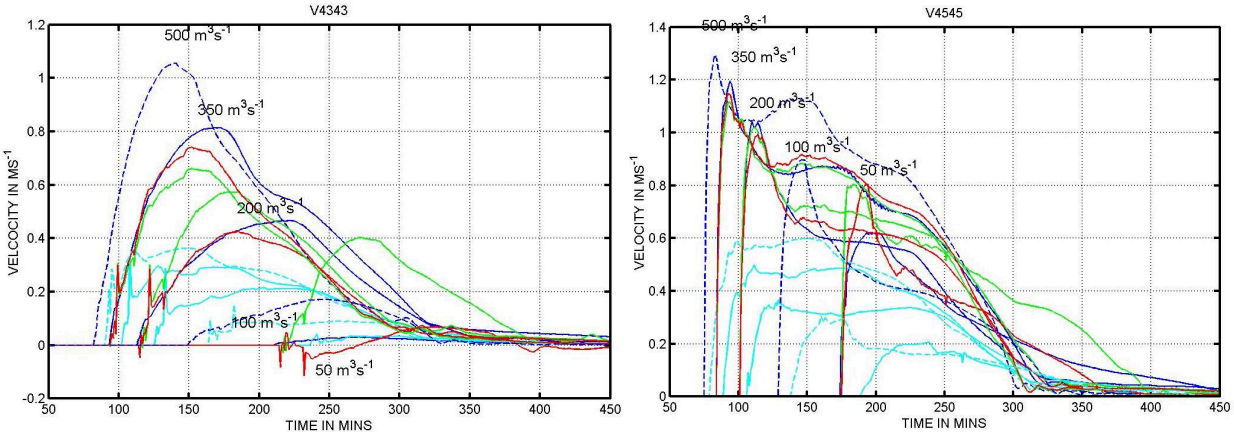

Figure 12. Prediction of velocity at 2 locations on the floodplain. Training runs based on q = 100 m^3/s and q = 500 m^3/s. See previous figure caption for colour codes.

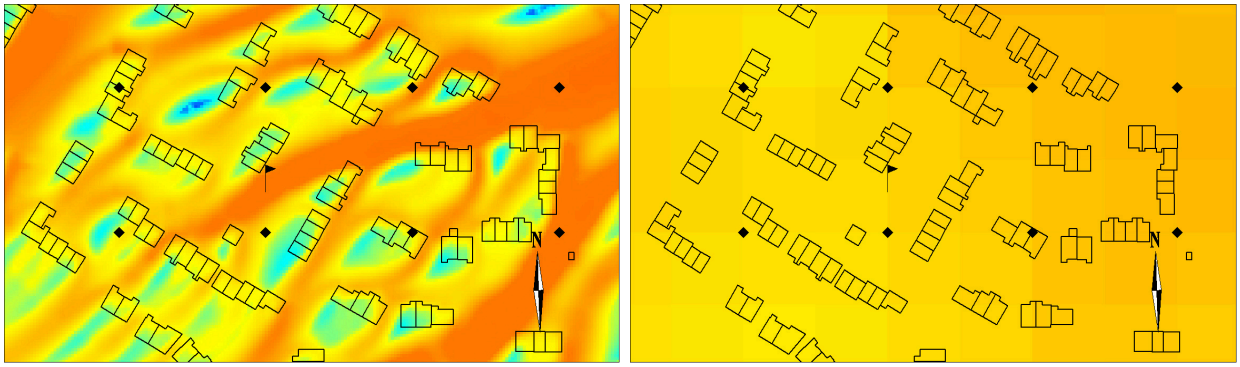

Figure 13. Peak velocity field predicted by a) the 2m FGM and b) the 50m CGM, for q = 200 m^3/s. the black dots are the computation nodes of the 50m model. The flag indicates the location where the approach is tested.

4.2 Improving spatial prediction of velocity

In addition to improving predictions of water levels and velocities at the computational grid points of the coarse grid model, the approach can also be used to improve the spatial resolution of CGM model results. Predictions at any location on the floodplain can be obtained by spatial interpolation from grid node predictions, and can subsequently be improved using an estimation of residuals. The inherent "blurring" effect obtained in the CGM predictions is illustrated by Figure 13, which clearly shows that major flow routes through the urban environment are not adequately modelled using the 50m model and that very significant benefits may be gained from using the results from training runs of the 2m models.

5. CONCLUSIONS

1. The increased availability of remotely sensed high resolution DEMs has led to an increase in the use of 2D models to simulate inundation arising from floods. Where RMS errors in the DEMs are limited to around 0.05 m vertical and 0.15 m horizontal these have little impact on model predictions, for higher RMS errors 0.15m vertical and 0.3m horizontal care must be taken to ensure these do not adversely influence model predictions.
2. Despite increased power of desk top computing facilities modellers are often required to compromise between model resolution and run-time. For the case study presented above it was possible to adjust roughness values in CGMs to account for sub-grid scale influence of buildings and other blockage effects.
3. CGM predictions of water depth and velocity can be improved to obtain predictions closer to those which would be obtained from a FGM by correcting the CGM results using residual differences between two FGM and CGM training runs.

REFERENCES

Bates, P.D. and De Roo, A.P.J. 2000 A simple raster-based model for flood inundation simulation. *Journal of Hydrology* 236: 54-77.

Chow, V.T. 1998. *Open Channel Hydraulics*. McGraw-Hill Education.

Cobby, D.M., Mason D.C., Horritt M.S. & Bates P.D. 2003. Two-dimensional hydraulic flood modelling using a finite-element mesh decomposed according to vegetation and

topographic features derived from airborne scanning laser altimetry. *Hydrological Processes* 17(10): 1979-2000.
Gomes Pereira L.M. & Wicherson R.J. 1999. Suitability of laser data for deriving geographical information. A case study in the context of management of fluvial zones. ISPRS Journal of Photogrammetry and Remote Sensing 54: 105-114.
Marks K. & Bates P.D. 2000. Integration of high-resolution topographic data with floodplain flow models. *Hydrological Processes* 14(11): 2109-2122.
Néelz S. P. F. and Pender G., "The influence of errors in digital terrain models on flood flow routes", River Flow 2006, Vol. 2, pp 1955 – 1962, Ferreira, Alves, Leal & Cardoso (eds), Taylor Francis, 2006,
Stelling, G.S. (1984). On the construction of computational methods for shallow water flow problems. *Rijkswaterstaat Communications,* No 35/1984. The Hague, Netherlands.
Syme, W.J. (1991). Dynamically Linked Two-Dimensional / One-Dimensional Hydrodynamic Modelling Program for Rivers, Estuaries & Coastal Waters. *M.Eng.Sc. (Research) Thesis*, Dept of Civil Engineering, The University of Queensland, Australia.

ACKNOWLEDGEMENTS

The research reported in this paper was conducted as part of the Flood Risk Management Research Consortium. The FRMRC is supported by grant GR/S76304 from the Engineering and Physical Sciences Research Council, in partnership with the Natural Environment Research Council, the DEFRA/EA Joint Research Programme on Flood and Coastal Defence, UKWIR, the Scottish Executive and the Rivers Agency (Northern Ireland). This financial support is gratefully acknowledged. The authors are also grateful to the Environment Agency for England and Wales, Infoterra and Halcrow Group Ltd. for providing the LiDAR data, to WBM Australia for the use of their TUFLOW software, and Ordnance Survey for providing Mastermap® data.